Towards bridging the gap between climate change projections and maize producers in South Africa

Willem A. Landman, [1]

Email Willem.Landman@up.ac.za

Francois Engelbrecht, [2,3]

Bruce Hewitson, [4]

Johan Malherbe, [2]

Jacobus van der Merwe, [2]

[1] Department of Geography, Geoinformatics and Meteorology, University of Pretoria, Private Bag X20, Pretoria, Hatfield, 0028 South Africa AQ2

[2] Natural Resources and the Environment, Council for Scientific and Industrial Research, Pretoria, South Africa

[3] Department of Geography, Archaeology and Environmental Studies, University of the Witwatersrand, Johannesburg, South Africa

[4] Climate System Analysis Group, University of Cape Town, Cape Town, South Africa

Abstract

Multi-decadal regional projections of future climate change are introduced into a linear statistical model in order to produce an ensemble of austral mid-summer maximum temperature simulations for southern Africa. The statistical model uses atmospheric thickness fields from a high-resolution (0.5° × 0.5°) reanalysis-forced simulation as predictors in order to develop a linear recalibration model which represents the relationship between atmospheric thickness fields and gridded maximum temperatures across the region. The regional climate model, the conformal-cubic atmospheric model (CCAM), projects maximum temperatures increases over southern Africa to be in the

order of 4 °C under low mitigation towards the end of the century or even higher. The statistical recalibration model is able to replicate these increasing temperatures, and the atmospheric thickness–maximum temperature relationship is shown to be stable under future climate conditions. Since dry land crop yields are not explicitly simulated by climate models but are sensitive to maximum temperature extremes, the effect of projected maximum temperature change on dry land crops of the Witbank maize production district of South Africa, assuming other factors remain unchanged, is then assessed by employing a statistical approach similar to the one used for maximum temperature projections.

1. Introduction

Global climate change is certain (IPCC 2014), and associated regional changes have also been manifesting across southern Africa (e.g. Kruger and Sekele 2013). Modelling efforts to simulate these and future changes over this region have subsequently increased and international programmes have been established in order to produce, among other outcomes, reliable high-resolution regional projections over multiple decades (e.g. Kim et al. 2014). These modelling efforts are being focused on both dynamic regional climate models and on statistical downscaling and recalibration methods (e.g. Maraun et al. 2010; Rummukainen 2010).

In South Africa, both statistical (Hewitson and Crane 2006; Hewitson et al. 2013) and dynamical downscaling (Engelbrecht et al. 2009, 2015) on multi-decadal time scales have been ongoing for a good number of years at local universities and institutions. In particular, the regional modelling capability at the Council for Scientific and Industrial Research has been developed around the conformal-cubic atmospheric model (CCAM; McGregor 2005; McGregor and Dix 2001, 2008). In fact, the CCAM has been applied to study southern African atmospheric dynamics over a wide range of time scales from daily weather variability to multi-decadal variations and change (Engelbrecht et al. 2011). Recently, the model was successfully used to realistically represent the strong temperature increases observed over southern Africa during the past five decades, and further significant warming was projected to occur during the twenty-first century (Engelbrecht et al. 2015). Furthermore, the study describes projected decreases in soil moisture availability even over regions where rainfall totals are projected to increase. Since the availability of sufficient soil moisture is important for high crop yields, and since the soil moisture may become deficient in a future climate due to increased temperatures, notwithstanding rainfall changes, rainfall as projected by the CCAM may therefore not be an ideal estimator for dry land crops for the decades ahead.

Over southern Africa, projections for the end of the century from multiple models suggest that the ensemble mean of these models is small compared to the natural internal rainfall variability of the region, but for temperatures, most models agree that the projections are large compared to its natural internal variability (IPCC 2014). Moreover, the response of climate models to greenhouse gas emissions is not equally certain for temperature and precipitation changes (Challinor et al. 2007) such that temperature-related phenomena (e.g. hot day frequency) are very likely to virtually certain to increase, while certain precipitation characteristics (e.g. rainfall amounts) may only be projected with medium confidence (IPCC 2014). This relatively low confidence in projected rainfall may make rainfall an unsuitable estimator of how crop yields may change in the future.

Owing to the "out of envelope" temperature projections over southern Africa towards the end of the century (Engelbrecht et al. 2015; IPCC 2014), the likely greater confidence of these projections over expected rainfall changes (IPCC 2014), and the expected decreases in soil moisture towards the end of the century as a result of temperatures increasing (Engelbrecht et al. 2015), it is clear that temperature is an important predictor to consider in projections of future crop yield over Africa (e.g. Thorncroft et al. 2011).

Here we introduce a statistical recalibration model that incorporates an ensemble of high-resolution CCAM output under low mitigation over multiple decades. We then test to see if the statistical recalibration model can adequately represented the "raw" CCAM projections of maximum temperatures over southern Africa and if the statistical relationships remain robust in a future climate. Finally, we generate statistical model projections of dry land crop yield under climate change.

2. Data and methods

2.1. Temperature and crop data

Monthly climatologies of the Climatic Research Unit (CRU) TS3.1 data set (Mitchell and Jones 2005) of the CRU are used for bias-correction of the regional climate simulations performed, while CRU TS3.1 December–January–February (DJF) maximum temperature data, averaged over the 3-month season, are used as one of the predictands in the statistical recalibration model presented.

We have chosen to use maximum temperatures since high temperatures are assumed to have major impact on yields, and it has already been shown over southern Africa that climate models are better able to simulate maximum temperatures as opposed to minimum temperatures (Lazenby et al. 2014) and by extension mean temperatures.

Observed production figures (yields) for dry land white and yellow maize are obtained from the South African National Department of Agriculture, Directorate: Statistics and Economic Analysis. Yearly yields are estimated from data obtained from producers and co-workers of the Department in the maize-producing areas of South Africa. Here we focus on the yields for the district of Witbank since statistical downscaling for seasonal-to-interannual yield production for this district has already been successfully demonstrated (Malherbe et al. 2014).

2.2. Regional climate model downscaling under a low mitigation future

CCAM is a variable-resolution global atmospheric model formulated on the conformal-cubic grid (McGregor 2005). The model can be applied at quasi-uniform resolution globally or in stretched-grid mode, using the Schmidt (1977) transformation, to obtain high-resolution output over an area of interest. In fact, variable-resolution global modelling provides a flexible framework for dynamic downscaling, so that in stretched-grid mode, the model effectively functions as a regional climate model. CCAM can firstly be integrated in stand-alone mode, functioning as quasi-uniform resolution or stretched-grid global model, when forced at its lower-boundary by sea-surface temperatures (SSTs) and sea-ice concentrations (SICs) from a host model or observations (Engelbrecht et al. 2009). Alternatively, the model can be spectrally nudged within the three-dimensional output of a host model or reanalysis (Thatcher and McGregor 2009, 2010; Engelbrecht et al. 2011), while more traditional grid-point nudging techniques can also be applied. In all these cases, for modestly stretched grids, the problems associated with the lateral boundary conditions of more conventional limited-area regional models are avoided (e.g. McGregor 2015). A detailed discussion of CCAM physics and configurations as applied in this paper are provided by Engelbrecht et al. (2011). For the research described here, six global circulation model (GCM) simulations (CSIRO Mk3.5, GFDL-CM2.0, GFDL-CM2.1, MIROC3.2-medres, ECHAM-MPI-ocean and UKMO-HadCM3) of the Coupled Model Intercomparison Project Phase 3 (CMIP3; Meehl et al. 2007), utilized in the AR4 of the IPCC, all obtained for the A2 SRES emission scenario, are dynamically downscaled to high resolution over southern Africa (referred to hereon as CCAM-AR4) for the period 1961–2100. A multiple nudging strategy is followed, by first integrating CCAM globally at quasi-uniform resolution (about 200 km resolution in the horizontal), forcing the model with the bias-corrected daily SSTs and sea-ice of each forcing model (Engelbrecht et al. 2015). In a second phase of the downscaling, CCAM is integrated in stretched grid mode with the area of highest resolution centred over southern Africa (28° E and 25° S) subsequently providing a resolution of about 60 km over the region. The higher resolution simulations were nudged within the quasi-uniform simulations, through the application of a scale-selective filter (Thatcher and McGregor 2009, 2010) using a 4000-km length scale. The filter was applied at six hourly intervals and from 900 hPa upwards and to the variables of temperature and the zonal and meridional wind components. The six CCAM-AR4 simulations are next interpolated, using a bicubic interpolation scheme, to the 0.5° latitude–longitude grid of the CRU data in order to facilitate the generation of gridded bias-corrected simulations. The generation of a bias-corrected version of the dynamic downscalings is important for their application to calculate indices relevant to biodiversity and agriculture (e.g. Engelbrecht and Engelbrecht 2015; Engelbrecht et al. 2015). However, these bias-corrections do not impact on the statistical recalibration procedure developed here, as the latter is based on atmospheric fields as the predictand (details to follow).

An important feature of the downscaling methodology described above is the use of only bias-corrected SST and SIC fields from the host GCMs as lower-boundary forcing in the downscaling process. Traditional downscaling procedures employ the raw SST fields as well as atmospheric forcing from the host models, and the CCAM methodology should therefore be regarded as enriching the ensemble of downscalings obtained through conventional limited-area model approaches. Details, advantages and disadvantages of the CCAM downscaling procedure applied here have been discussed in detail by Katzfey et al. (2009), Nguyen et al. (2012) and Engelbrecht et al. (2015). Biases are calculated by comparing the monthly GCM climatologies over the period 1961–2000 to the corresponding Reynolds (1988) SST climatologies. The identified biases are removed consistently from the GCM fields for the entire simulation period 1961–2100. This procedure preserves the interannual variability and climate change signal of the raw GCM SSTs, but typical GCM biases in the representation in SSTs on the African west coast and the equatorial Pacific SSTs (the cold tongue bias) are removed. The procedure has been shown to produce better present-day climatologies in CCAM simulations compared to simulations where raw SSTs and atmospheric fields from the host models are used as forcing (Katzfey et al. 2009)—note in particular that GCMs suffering from significant SST biases in the Pacific often also exhibit significant distortions in their simulations of the trade winds over the Pacific. A feature of these simulations is thus that the RCM (CCAM) can simulate atmospheric flow patterns not consistent with that of the forcing GCM. To a large extent, this bias correction procedure results in atmospheric model simulations very similar in nature to that outlined by the Atmospheric Model Intercomparison Project (AMIP). In particular, AMIP simulations using CCAM and a variety of atmosphere-only GCMs have been demonstrated to be able to simulate the most important teleconnection to southern African climate, namely ENSO (e.g. Engelbrecht et al. 2011). Bias-correcting the tropical SSTs to realistically represent ENSO SST patterns is therefore arguably more important than the inconsistencies that may develop in the tropics between atmospheric fields forced by SST.

2.3. Statistical recalibration model

A 31-year reanalysis simulation using CCAM was applied on the same stretched-grid providing 60 km resolution data over southern Africa (Engelbrecht et al. 2011), with the difference that the simulations were nudged within NCEP II reanalysis data (Kalnay et al. 1996), rather than the output fields of GCMs (this data set will be referred to from here on as "CCAM-rea"). The settings of the digital filter applied in the nudging procedure were exactly as for the CCAM-AR4 downscalings. The simulations were performed for the period 1979–2009. The model output, available at 6-hourly intervals, was subsequently interpolated onto the 0.5° latitude–longitude grid employed by the CRU TS3.1 data set. A 30-year time series of DJF-averages for the seasons 1979/1980 to 2008/2009 is subsequently calculated and used as predictors in the statistical recalibration model with the focus on southern Africa. Specifically, the predictors of maximum temperatures are the CCAM-rea's DJF thickness fields (averaged over all days per DJF season) as represented by the geopotential height differences between the 850 and 500 hPa levels. The 850 hPa pressure level is the most representative of the low-level circulation over the interior of southern Africa and approximates the height of the South African central plateau (Riphagen et al. 2002). For certain areas where elevations over the interior is greater than the standard height of the 850 hPa pressure level, the relevant CCAM grid-point values are extrapolated to the 850 hPa level through the hypsometric equation and assuming a standard lapse rate of 6.5 °C/km. Take note that the highest elevation regions in South Africa reach the 700 hPa level but that circulation at this height (about 3000 m) is not representative of the low-level synoptic scale flow over most of the interior.

The thickness of the layer between two isobaric surfaces is proportional to the mean temperature in the layer through the hypsometric relationship (Holton and Hakim 2013). As the layer warms and cools, the thickness of that layer changes in response—a warming layer has its thickness increasing; a cooling layer is associated with decreasing thickness. Therefore, instead of statistically linking the simulated maximum temperatures of the CCAM directly to observed maximum temperatures, we are interested to find out if the atmospheric dynamics and thermodynamics of the CCAM, as represented by thicknesses, can relate to a surface variable such as maximum temperatures. The DJF maximum temperature used as predictand in the statistical recalibration model are the CRU-gridded data mentioned above. The statistical model is created by the canonical correlation analysis (CCA) option of the Climate Predictability Tool (CPT; Mason and Tippett 2016). CCA and principal component regression (PCR) have already been used extensively for southern African climate studies, including a CCA study on maximum temperature seasonal variations and predictability (Lazenby et al. 2014) and a PCR model for predicting seasonal crop yields (Malherbe et al. 2014).

The predictor domain is the area between the equator and 45° S and between 15° W and 60° E; the predictand domain is between 12° and 35°S and 11° to 41°E. Empirical orthogonal function (EOF) prefiltering is first performed with nine selected as the maximum number of predictor and predictand EOF and CCA modes allowed in the model. Cross-validation is performed next and the recalibrated simulations compared with observed (CRU) maximum temperatures. In order to minimize the chance of obtaining biased results, a large leave-5-year-out window is used in the cross-validation process (e.g. Landman et al. 2014). The Spearman rank correlation between observed and simulated maximum temperatures is calculated for each grid-point. The median, 85th and 99.9th percentile values of the Spearman correlations at all the grid-points are respectively 0.64, 0.72 and 0.82, and these high values indicate that the CCA procedure relating the DJF thickness fields with the observed maximum temperatures are adequate. Figure 1 further demonstrates the close association between statistically recalibrated maximum temperature simulations and the observed maximum temperatures. The figure shows the area-averaged recalibrated and area-averaged observed DJF maximum temperatures over 30 years (1979/80–2008/09) with a Spearman rank correlation between the two time series of 0.86.

Fig. 1

Area-averaged cross-validated recalibrated (*dashed line*) and observed (*solid line*) maximum temperatures over *SADC* during *DJF*. CCAM-rea 850–500 hPa thickness fields are used as predictor. The Spearman rank correlation between the two time series and its level of statistical significance are presented at the *bottom left* of the plot

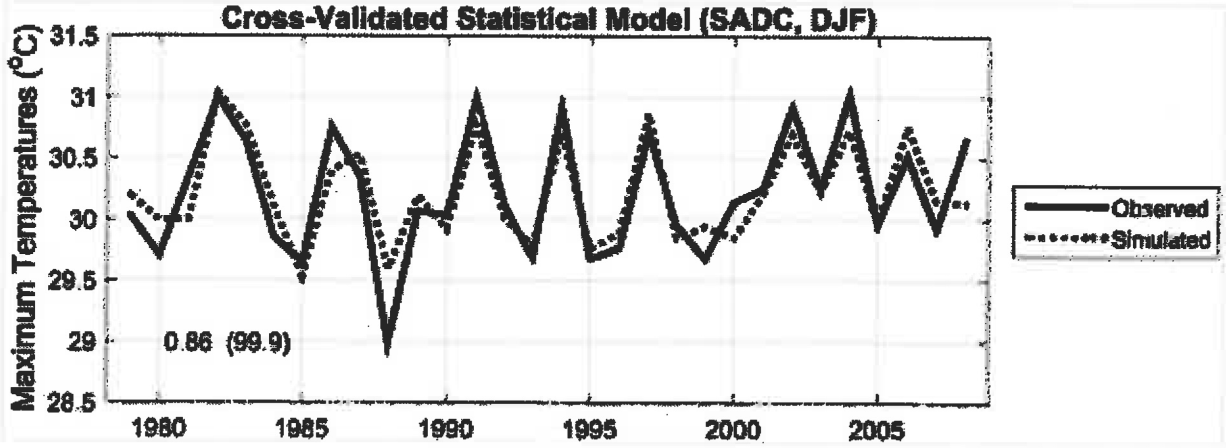

The CCA procedure that produced the results represented in Fig. 1 is then used to recalibrate the six AR4 projections over multiple decades. Figure 2 shows the statistical recalibration procedure schematically: CCAM-rea (DJF thickness fields) and observed data (DJF CRU maximum temperatures) are used to develop the statistical recalibration model as described above; the CCAM-AR4 fields (DJF thickness fields) are subsequently used in the CCA to produce statistically recalibrated DJF maximum temperature projections over multiple decades.

Fig. 2

The three steps to statistically recalibrate over multiple decades. The first step (*1*) is to develop a statistical downscaling model using CRU maximum temperatures as predictand and the CCAM-rea (downscaling of the NCEP reanalysis) as predictor (850–500 hPa thickness fields). The second step (*2*) is to obtain the projected CCAM-AR4 thickness fields and the third step (*3*) is to statistically recalibrate to maximum temperatures over 139 years by using the CCAM-AR4 thicknesses as predictor

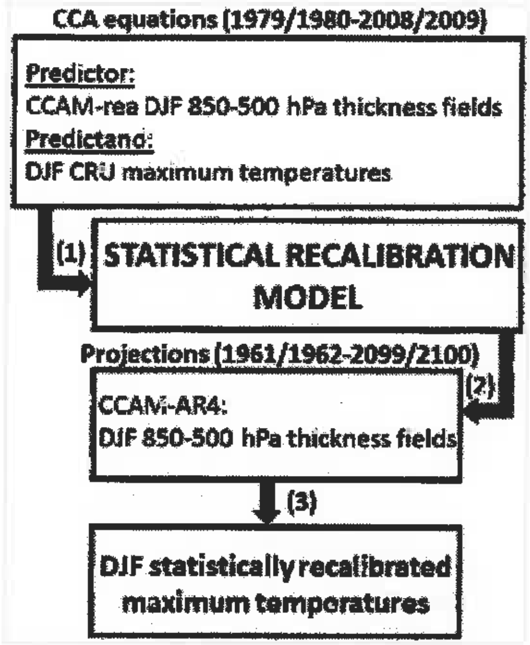

In order to form an understanding of the physical aspects of the statistical model, we perform CCA pattern analysis (Barnett and Preisendorfer 1987) over the period from which the statistical model is derived. CCA is first performed to compare the space-time evolution of (1) the respective thickness fields (850–500 hPa) of the coarse-resolution NCEP reanalysis with the higher resolution CCAM-rea data and of (2) the predictor (CCAM-rea; 850–500 hPa thickness fields) with predictand variables (CRU maximum temperatures) used in the statistical recalibration model. Figure 3 shows a strong agreement between the NCEP and CCAM-rea data, which provides evidence that the high-resolution DJF seasonal data produced by the CCAM is closely similar to the DJF NCEP data—for all three modes presented here, the canonical time scores (middle panels) are highly correlated and the corresponding spatial patterns of the CCAM-rea and NCEP are very similar. Although only the first three modes are presented, the agreements per mode are found across all modes considered.

Fig. 3

CCA spatial and temporal representations of the linear association between NCEP's and CCAM-rea's 850–500 hPa thickness fields for the DJF season. The *top row* represents *mode 1*, the *middle row mode 2* and the *bottom row mode 3*. For the temporal scores, NCEP is represented by *open circles* and CCAM-rea by *crosses*. The canonical correlations are respectively 0.9996, 0.9915 and 0.9894. Years refer to the Decembers of the DJF seasons

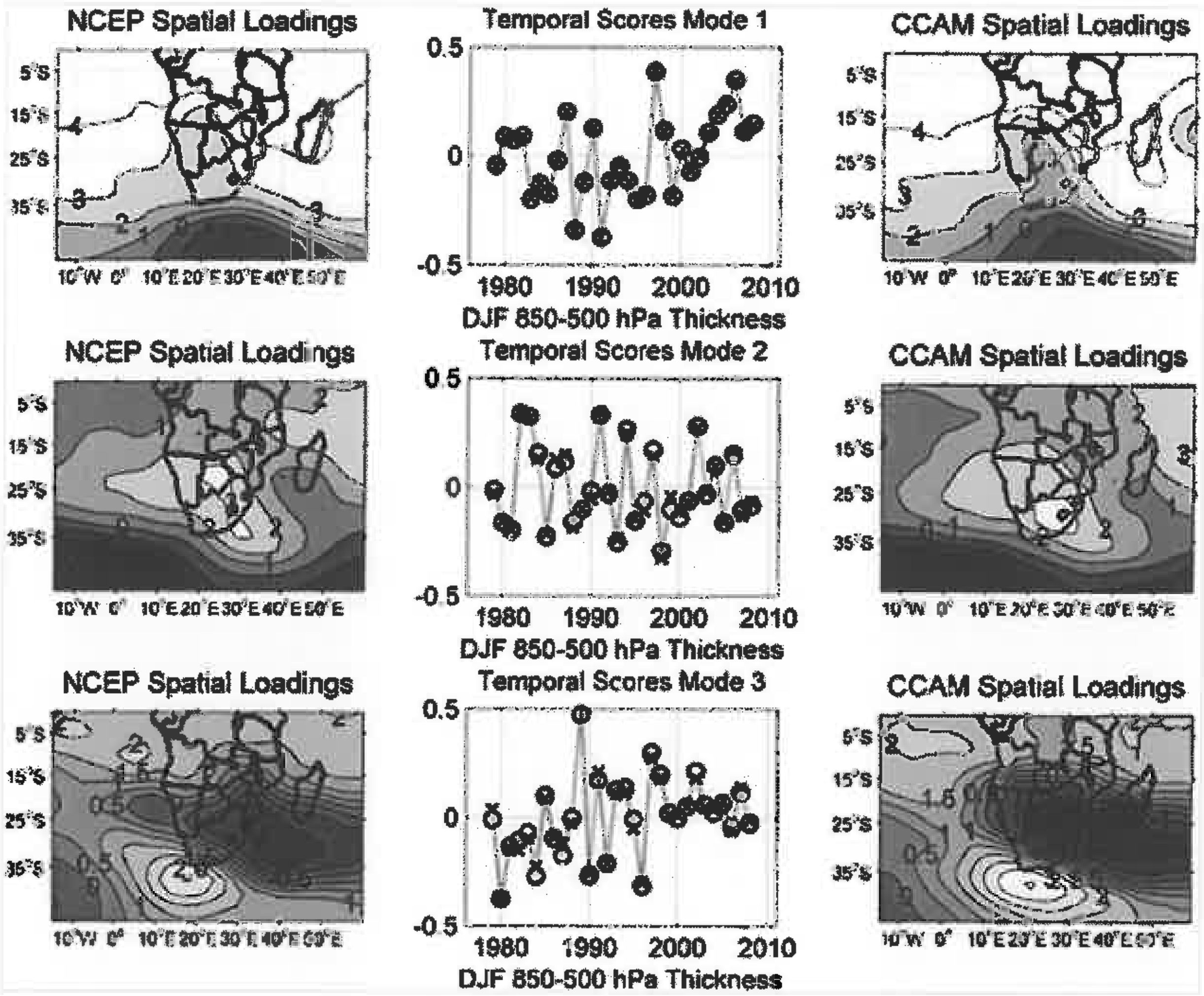

The reason why the CCAM-rea data are subsequently used in the statistical model instead of simply interpolating 2.5° resolution NCEP data to the higher resolution or to use other current high-resolution reanalysis is to ensure dynamical consistency when developing these equations, since the 0.5° resolution CCAM-AR4 projections are to be used in the statistical recalibration model developed with CCAM-rea data (Fig. 2). Because CCAM output is used for both the statistical equation development stage and for statistical recalibration over multiple decades, a more consistent representation of the climate system is produced since, among others, the parameterization schemes as well as the dynamical core are the same throughout. For example, should the atmospheric model have a tropospheric temperature bias due to say, systematic errors in aerosol radiation interactions, the thickness bias is likely to be similar in both CCAM-rea and CCAM-AR4 downscalings.

Figure 4 shows CCA analysis of the predictor and predictand DJF seasonal fields used for developing the statistical recalibration model, i.e. the 850–500 hPa DJF thickness fields of the CCAM-rea data (predictor) and the CRU DJF maximum temperatures (predictand) on the land-surface. The strong linear association (high canonical correlations) between the atmospheric thickness and surface maximum temperatures can be seen in the figure. Of particular interest are the patterns of the first, and most dominant, mode of Fig. 4—this mode is very similar to the second mode of the thickness fields of Fig. 3. For the first and dominant mode of Fig. 4, when DJF thicknesses are anomalously high (low) over southern Africa and adjacent oceans, anomalously high (low) DJF maximum temperatures on the surface are found over the larger part of southern Africa. The statistical recalibration model is thus based primarily on this premise: DJF thickness of the lower atmospheric layer above southern Africa is directly proportional to the DJF maximum temperatures on the surface.

Fig. 4

CCA spatial and temporal representation of the linear association between CCAM-rea 850–500 hPa thickness fields and gridded CRU maximum temperatures during DJF. The *top row* represents *mode 1*, the *middle row mode 2* and the *bottom row mode 3*. For the temporal scores, CCAM-rea is represented by *open circles* and the CRU maximum temperatures by *crosses*. The canonical correlations are respectively 0.9175, 0.7497 and 0.6585. Years refer to the Decembers of the DJF seasons

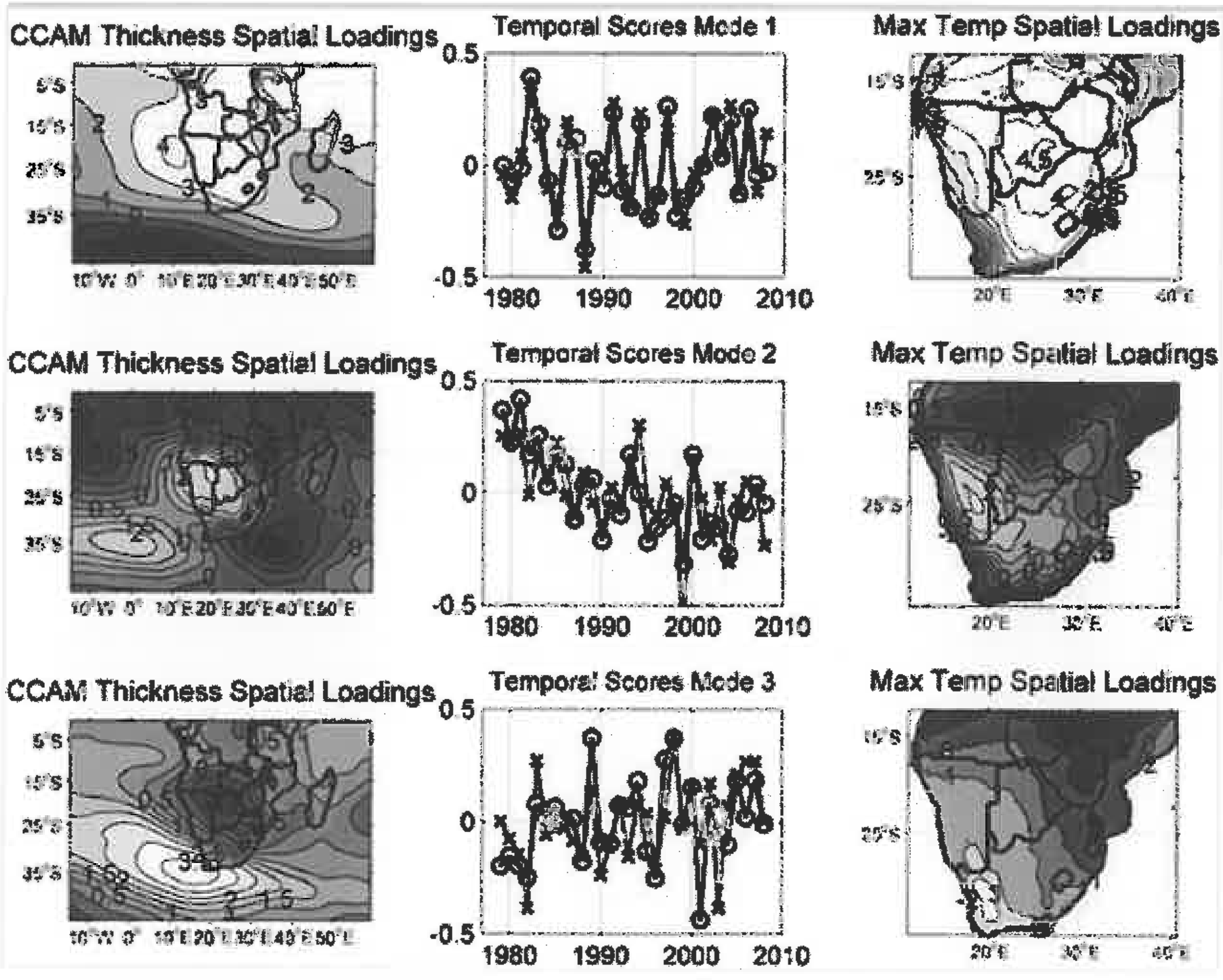

The CCA-based statistical model is subsequently used to recalibrate the DJF maximum temperature fields over 139 years from 1961/1962 to 2099/2100 and for each of the six CCAM-AR4 projections in order to produce an ensemble of statistically post-processed projections. The statistically projected DJF maximum temperature data averaged over the 30-year present-day climate period from 1961/1962 to 1990/1991 are compared with averaged CRU maximum temperatures over the same period in order to calculate an estimate of the offset of each of the six projections at each grid-point. On average, the projections over the present-day period are about 1 °C too warm. This may suggest the existence of a positive bias in the CCAM-AR4 downscalings in terms of 850 to 500 hPa thickness. This offset is subsequently corrected over the entire 139-year period and for each simulation, a step that corresponds to the bias-correction of the dynamically downscaled temperatures is described in Sect. 2.2.

2.4. Statistical crop yield models

The statistical recalibration approach presented for maximum temperatures is similarly applied to crop yields: 850–500 hPa DJF thickness fields of the CCAM are used as predictor in a statistical model, but this time, PCR is used instead of CCA to develop the statistical equations since the model is developed only for a single location as opposed to an area that includes various locations or grid-points when using CCA. Other than this difference, the approach is effectively the same: The same predictor domain and the same predictor (thicknesses) are used and also a 5-year-out cross-validation window to develop and test the statistical crop yield model. Another subtle difference is that the period over which the crop yield model is developed is over 29 years (end-of-season yields for the period 1981 to 2009) as opposed to the 30-year period used before for maximum temperature recalibration (DJF 1979/80 to 2008/09).

We also developed a statistical crop yield model based on the 850 hPa geopotential height field of the CCAM. This low-level circulation parameter as produced by GCMs has on a number of occasions been used successfully in statistical models to recalibrate (Landman and Goddard 2002) and downscale seasonal rainfall forecasts over southern Africa (Landman and Beraki 2012) and can therefore be considered as a proxy for seasonal rainfall totals observed on the ground. In addition to the seasonal rainfall forecast models, the 850 hPa heights of a GCM have also been used to produce seasonal crop yield forecasts for South Africa (Malherbe et al. 2014). This second statistical crop yield model is set up in exactly the same way as the abovementioned thickness-based statistical crop yield model. The reason for developing the additional model is to produce rainfall-based downscaled crop yields for a future climate, when the temperature-rainfall relationship may be different to what is known for the present-day climate, with the only purpose to compare the projections of the two crop yield models.

2.5. Approach summarized

In order to summarize the approach to produce projections of end-of-season crop yield for the Witbank area, the following steps are executed:

- Two CCAM data sets are used: the CCAM-rea to develop statistical models and the CCAM-AR4 6-member ensemble to provide predictors for the statistical models for recalibration and downscaling for a future climate.

- We have shown above that CCAM-rea thickness is a good proxy for observed maximum temperatures at the surface through CCA pattern analysis. Next, it will be tested if the CCAM-AR4 thicknesses can be successfully used in a statistical model to replicate an ensemble of raw CCAM-rea maximum temperature projections. The reasons why the greater focus is on maximum temperatures and not on rainfall is because of the enhanced confidence that exists in the projections of the former as opposed to the latter, because of the virtual certainty that temperatures in a future climate over southern Africa are expected to be well-beyond its present-day average and because of the probable link between maximum temperatures over the summer season and end-of-season Witbank crop yields.

- A statistical crop yield model will subsequently be developed and tested for downscaling to Witbank present-day and future crops by using CCAM thickness (the maximum temperature proxy) as predictor. A circulation-based statistical model is additionally developed in order to ascertain the influence of seasonal rainfall on future crop yields and to compare it with the maximum temperature based crop model output.

3. Results

3.1. Maximum temperature recalibration over southern Africa

As two time series over the 139 years, Fig. 5 shows the area-averaged ensemble mean (over the six projections) of both the CCAM-AR4 and statistical recalibration model temperature projections. A second-order polynomial is separately applied to each time series for the sole purpose of visualization. A close resemblance between the two projections is evident (both show a warming non-linear trend and the Spearman rank correlation between the two varying time series is 0.95) which suggests that the statistical downscaling model that uses a thermodynamic field (the 850–500 hPa thickness) as predictor is a good representation of raw CCAM-AR4 output, and both projections suggest that southern Africa may experience +4 °C warming in maximum temperatures by the end of this century (e.g. Engelbrecht et al. 2015). Such a warming has been proposed in the literature (e.g. Greene et al. 2006) and will require substantial shifts in agricultural practices (Thornton et al. 2011) since the likelihood of increases in the occurrence of warm temperature extremes will likely continue to increase worldwide, leading to significant impacts on agriculture (Weaver et al. 2014). Our result is evidence that the statistical recalibration model is robust, and is particularly encouraging since atmospheric thickness fields (a more robust parameter of models) and not the CCAM's raw maximum temperature projections are used as predictors in the statistical model.

Fig. 5

Area-averaged ensemble mean of both the CCAM-AR4 and statistical recalibration model DJF maximum temperatures. Simulations for each year and for fitted polynomials are presented

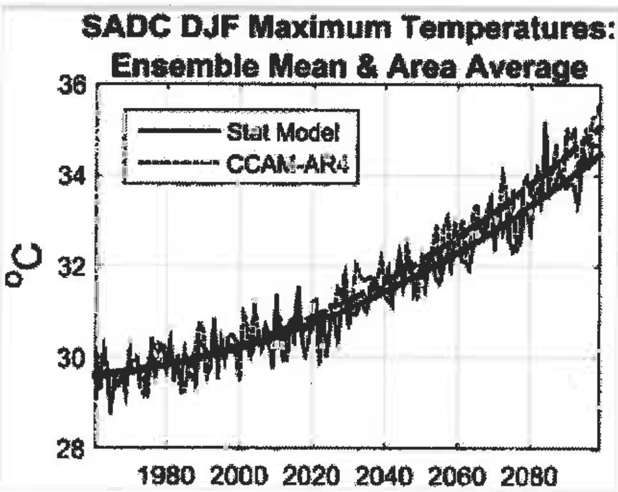

The statistical model presented here does not necessarily improve (although it shows slightly different outcomes) on the CCAM-AR4 output. Take note that our motivation to develop this statistical recalibration model that may be able to replicate the output from a regional climate model is to produce climate projections of variables not explicitly simulated by models but whose variation may be strongly linked to climate variations, in this case crop yield. In addition, by comparing the recalibrated output with the CCAM-AR4 output may be a very useful example of a pseudo reality experiment to check whether the predictors capture climate change. For this purpose, insight into the spatial description of the extent to which the statistical model is replicating the raw model output may be useful and is shown in Fig. 6. The present-day climate patterns of both modelling systems (top panels of Fig. 6) are in strong agreement. However, some differences are evident over the 2070/2071 to 2099/2100 periods (bottom panels of Fig. 6) mostly over the western-central and over the far northern parts where the statistical method respectively simulates DJF maximum temperature climates warmer and cooler relative to the raw CCAM-AR4 data.

Fig. 6

Ensemble mean 30-year climates of CCAM-AR4 (*left panels*) and of the statistical recalibration model (*right panels*) DJF maximum temperatures

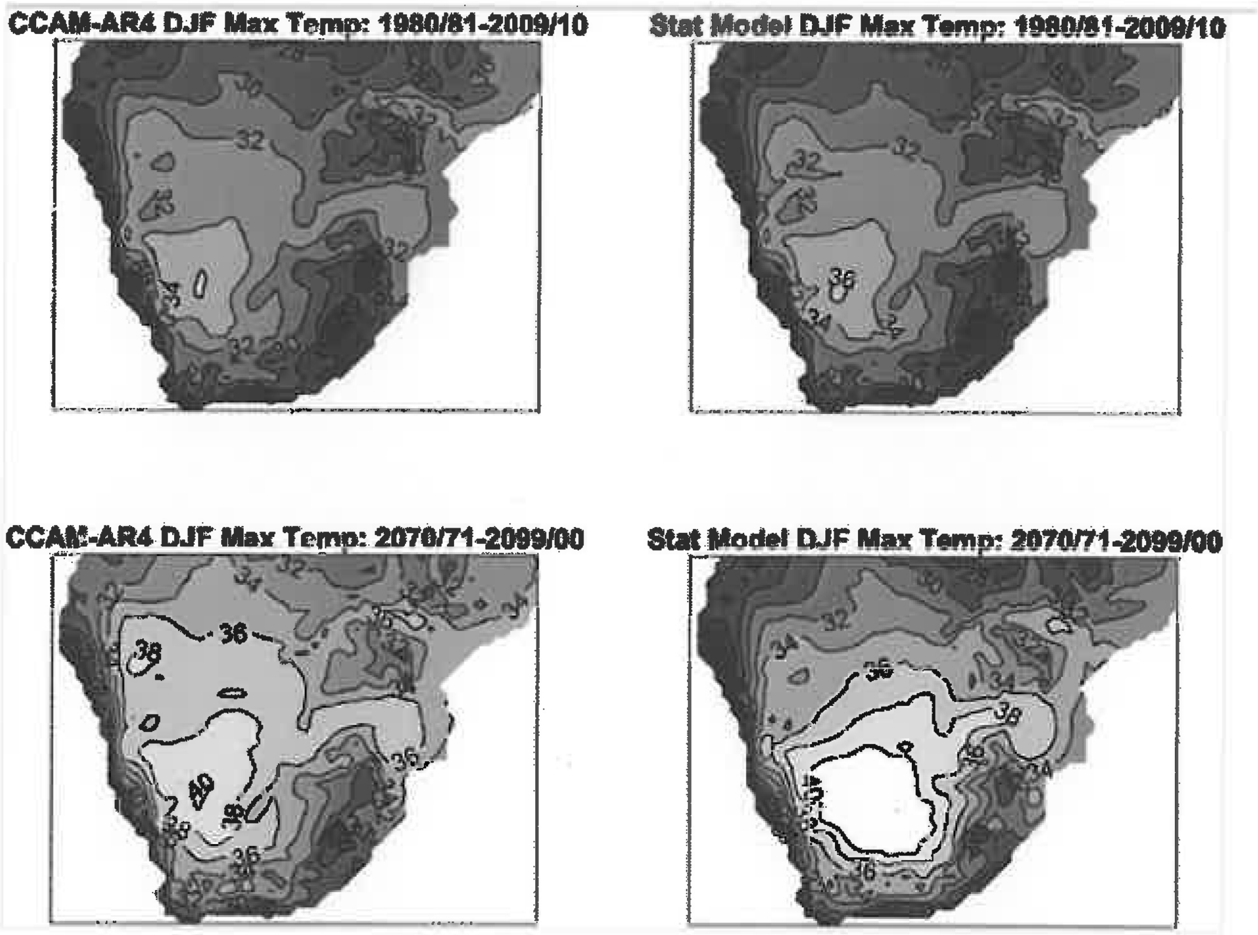

3.2. Stationarity of statistical relationships

The developed statistical relationships between the seasonal thickness fields as predictor and the maximum temperatures as predictand are inherently assumed to remain valid under future climate conditions and also that the future trends of the fields are well represented by both the CCAM and the statistical model. Figure 7 explores this assumption and shows the 850–500 hPa thicknesses vs. maximum temperatures, averaged over the southern African domain, and averaged over the six projections and over four 30-year periods. For both the CCAM-AR4 projections and for the statistical recalibration model, increasing atmospheric thickness in a future climate is associated with increasing maximum temperatures. This positive association between thickness and maximum temperatures remains robust throughout the multi-decadal integration period, and so supports the assumption that the statistical downscaling model that incorporates CCAM-AR4 thickness fields should be able to produce reliable recalibrated maximum temperature projections from these thickness fields over the whole multiple decade period.

Fig. 7

Ensemble mean area- (southern Africa) and time-averaged (over the 30-year periods as shown on the figure) DJF maximum temperatures vs. DJF atmospheric thickness fields. For both the CCAM-AR4 projections (*asterisks*) and for the statistical recalibration model (*open circles*), increasing atmospheric thickness in a future climate is associated with increasing maximum temperatures

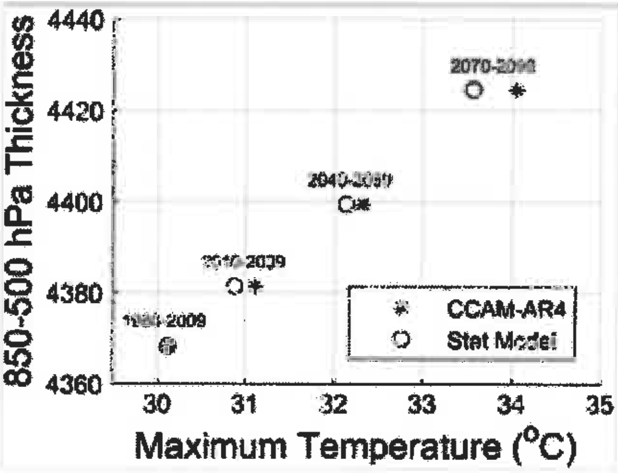

3.3. Projections applied: statistical crop yield estimates

Strong agreement among the CCAM-AR4 and the statistical recalibration model's projected climates (Fig. 6) is found for the eastern Highveld of South Africa where the maize production districts of Witbank are located. A PCR statistical recalibration model is subsequently applied to Witbank dry land maize yields using CCAM thicknesses as predictor. DJF maximum temperatures, represented here by DJF atmospheric thickness fields as described above, may be considered as a proxy for dry land maize production since intense heat may lead to increased evapotranspiration which in turn adds stress to the development of dry land maize crops. In addition, the early stages of crop growth are not as critical as during tasseling and grain-filling (Mjelde et al. 1997) which typically occurs during mid-summer (i.e. DJF), hence the focus on the DJF season. During this season, higher than normal temperatures can therefore cause heat stress-related impacts while the associated increased evapotranspiration can create large negative values in the water balance that will consequently result in lower end-of-season yields.

The relationship between DJF thickness fields with dry land crops is further demonstrated by developing and testing a PCR model of the CCAM-rea's DJF

850–500 hPa thickness fields as a predictor of Witbank's detrended end-of-season maize yield. A leave-5-year-out cross-validation over 29 years (1981 to 2009) is used, and Spearman rank correlation between simulated and observed yields of 0.39 ($p < 0.02$) is subsequently found. Figure 8 shows cross-validated simulations (from the statistical PCR model) vs. observed end-of-season maize yield indices (normalized values). The absolute errors between the simulated and observed yields are also shown on the figure. The two largest errors are seen for the 1999 and 2001 yields, both La Niña seasons (as defined by the Oceanic Niño Index—http://www.cpc.ncep.noaa.gov/products/analysis_monitoring/ensostuff/ensoyears.shtm), when negative yield anomalies are observed but the simulated anomalies are positive. Excluding these 2 years from the analysis increases the Spearman correlation to 0.52 (significant at the 99.7% level). Drought conditions occurred during these years with associated high temperatures during some of the summer months, notwithstanding the presence of a La Niña event. The presence of a tropical low over Mozambique during February 1999 confined above-normal rainfall towards the east of the maize-production region while hot and dry conditions occurred across much of central South Africa during this very sensitive maize growth period. In 2001, similar circulation patterns also resulted in dry conditions over much of the summer rainfall region of South Africa while above-normal rainfall occurred in the vicinity of tropical systems located close to the north-eastern extremes of the country. However, positive yield anomalies are simulated and observed for the La Niña seasons of 1989, 1996, 2000 and 2008, while negative anomalies are simulated and observed during the El Niño seasons of 1983, 1992, 1995, 1998, 2003 and 2007. The result that the statistical model captured the correct sign of the yield anomaly for the majority of El Niño and La Niña cases (10 out of 16 events over the PCR development period—62.5%) is of significance because we might possibly experience a near-doubling of extreme El Niño and La Niña occurrences in response to greenhouse warming (Cai et al. 2014, 2015). However, the relatively low Spearman correlations mentioned above and that yields are not always accurately simulated for every La Niña and El Niño season may undermine the PCR downscaling model to reliably project decadal changes in maize yield and as a result add to the uncertainties of these projections. Figure 8 also shows yield simulations when using the DJF low-level 850 hPa circulation (a proxy for rainfall) as predictor (thin solid line). Although this rainfall yield model produces slightly different results, the Spearman rank correlation between the two statistical model simulations using respectively thickness and low-level circulation as predictor is 0.75 indicating that it is capturing the core aspects.

Fig. 8

Cross-validated statistically downscaled (*dashed line*—using thicknesses as predictor; *thin solid line*—using low-level circulation as predictor) and observed (*thick solid line*) end-of-season maize yield indices for the Witbank region. The *circled asterisks* show the absolute errors only between simulations based on thickness fields and observations per year. The *numbers* near the *bottom* on the figure are the Spearman rank correlations and their levels of statistical significance (from *left* to *right*) between the observed and thickness-based simulation, the observed and circulation-based simulation and between the two simulations

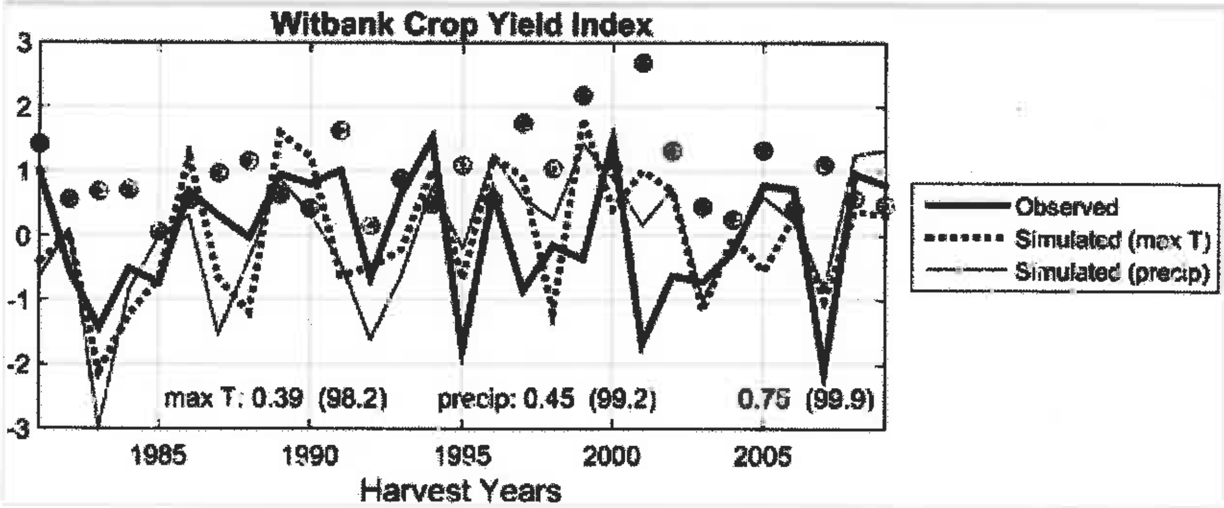

The PCR model is next applied for dry land crop projections over 139 years by using as predictors the (1) DJF 850–500 hPa thickness simulations and (2) the DJF 850 hPa geopotential height simulations of the six CCAM-AR4 projections. Offset adjustments on the simulated yields are performed similar to the adjustment procedure explained above for maximum temperatures but with a maize yield present-day climate period of 1981 to 2009. Figure 9 shows the dry land maize yield projections at Witbank. All six maximum temperature-based downscaled projections for each year are shown together with a second-order polynomial fitted to the average of the six projections (thick solid line). Also presented in Fig. 9 is the polynomial of the average of the six rainfall based projections, which effectively is a straight line (thick dashed line).

Fig. 9

Projections by the PCR statistical models of Witbank dry land maize yields. Thickness-based (maximum temperatures) downscaled values for each year and for a polynomial fitted to the averaged projections are presented. For low-level circulation (rainfall), only the polynomial fitted to its averaged projections is presented (*thick dashed line*). The driving IPCC models are listed on the right. The years on the *x*-axis refer to the year of harvest, typically in March

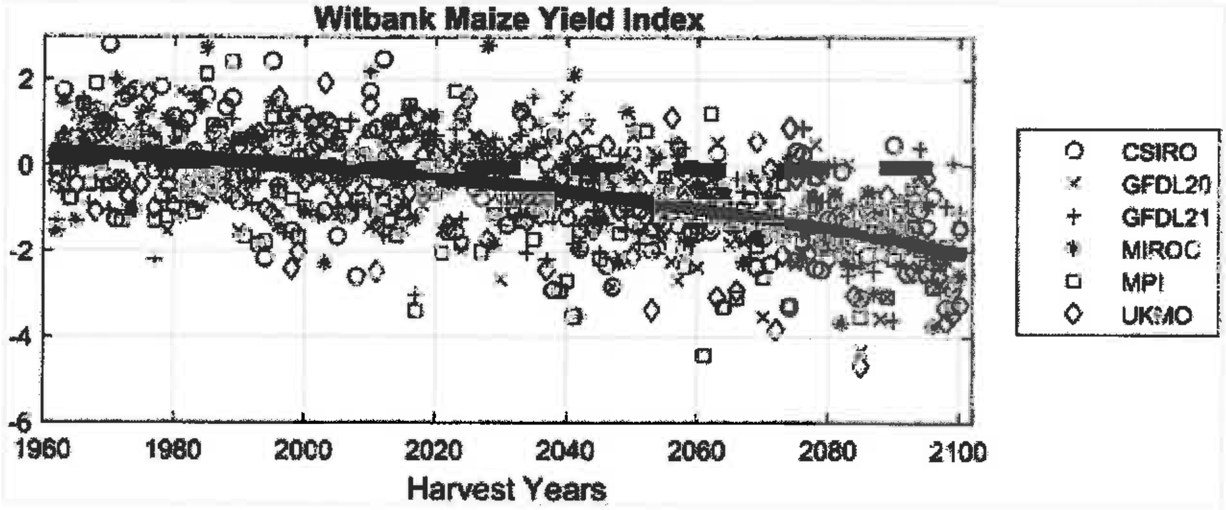

The downscaling procedure that uses thicknesses as predictor is simulating on average a reduction in dry land maize yield over the Witbank area of about two standard deviations by the end of this century—a substantial reduction in crop yield associated with the projected increase of mid-summer maximum temperatures. On the other hand, the downscaling using low-level circulation (rainfall proxy) as predictor simulates no apparent changes on average in crop yields towards the end of the century. Which one of the two projections is to be deemed more realistic is difficult to assess. However, the reduced crop yield simulation may be more realistic since the dry land maize plant will be subject to increased evapotranspiration associated with the virtually certain increased maximum temperatures and expected decreases in soil moisture projected towards the end of the century. Take note that the results assume no changes in farming practices or maize varieties used. Moreover, from Fig. 9, it is evident that the projections are associated with a considerable amount of uncertainty on exactly how much the yield may be reduced under A2 SRES as reflected by the range of possible projected outcomes.

4. Conclusions

Climate change adaptation in southern Africa for maize yield would require higher tolerance of maximum temperatures in existing maize varieties or a change in the varieties of maize grown in the region (Thornton et al. 2011). Here we focus on the former and subsequently developed a statistical downscaling procedure to objectively simulate a commodity sensitive to temperature extremes, such as dry land crops, over multiple decades.

First it was shown that a statistical recalibration model applied to regional climate model outputs is able to capture the regional climate models' upward trends in maximum temperatures over southern Africa during mid-summer and that the relationship between atmospheric thickness and maximum temperatures remains robust in a future climate. We were therefore able to develop a statistical procedure that could replicate output from a regional climate model. Such a procedure can then potentially be used to simulate variables or commodities not produced explicitly by a climate model, such as dry land crops.

The statistical simulation through downscaling of crop yields over multiple decades was subsequently performed, and it was found that yields may be reduced on average by the end of this century. This result is of course based on the assumption that the maize cultivars are not genetically enhanced and that the projections are highly certain and for a low mitigation A2 SRES future. Moreover, there are additional uncertainties associated with this approach as a result of the still imperfect statistical equations that lead to simulated crops which are associated with a large spread of possible outcomes. What may be much less uncertain is that with the projected increase of temperatures, it seems unlikely that crop yields may increase as a result over the coming decades. The procedure described here may therefore at least be able to provide some guidance to policy makers responsible for action plans to mitigate and adapt to the impacts of increasing temperatures on dry land maize yield.

Acknowledgments

This material is based upon work partly supported financially by the National Research Foundation of South Africa and by the Applied Centre for Climate and Earth System Science.

References

Barnett TP, Preisendorfer RW (1987) Origins and levels of monthly and seasonal forecast skill for United States air temperature determined by canonical correlation analysis. Mon Weather Rev 115:1825–1850

Cai W, Borlace S, Lengaigne M, van Rensch P, Collins M, Vecchi G, Timmermann A, Santoso A, McPhaden MJ, Wu L, England MH, Wang G, Guilyardi A, Jin F-F (2014) Increasing frequency of extreme El Niño events due to greenhouse warming. Nat Clim Chang. doi: 10.1038/NCLIMATE2100

Cai W, Wang G, Santoso A, McPhaden MJ, Wu L, Jin F-F, Timmermann A, Collins M, Vecchi G, Lengaigne M, England MH, Dommenget D, Takahashi K, Guilyardi E (2015) Increased frequency of extreme La Niña events under greenhouse warming. Nat Clim Chang. doi: 10.1038/NCLIMATE2492

Challinor A, Wheeler T, Garforth C, Craufurd P, Kassam A (2007) Assessing the vulnerability of food crop systems in Africa to climate change. Clim Chang 83:381–399. doi: 10.1007/s10584-007-9249-0

Engelbrecht CJ, Engelbrecht FA (2015) Shifts in Köppen-Geiger climate zones over southern Africa in relation to key global temperature goals. Theor Appl Climatol. doi: 10.1007/s00704-014-1354-1

Engelbrecht FA, McGregor JL, Engelbrecht CJ (2009) Dynamics of the conformal-cubic atmospheric model projected climate-change signal over southern Africa. Int J Climatol 29:1013–1033

Engelbrecht FA, Landman WA, Engelbrecht CJ, Landman S, Bopape MM, Roux B, McGregor JL, Thatcher M (2011) Multi-scale climate modelling over southern Africa using a variable-resolution global model. Water SA 37:647–658

Engelbrecht F, Adegoke J, Bopape MM, Naidoo M, Garland R, Thatcher M, McGregor J, Katzfey J, Werner M, Ichoku C, Gatebe C (2015) Projections of rapidly rising surface temperatures over Africa under low mitigation. Environ Res Lett. doi: 10.1088/1748-9326/10/8/085004

Greene AM, Goddard L, Lall U (2006) Probabilistic multimodel regional temperature change projections. J Clim 19:4326–4343

Hewitson BC, Crane RG (2006) Consensus between GCM climate change projections with empirical downscaling: precipitation downscaling over South Africa. Int J Climatol 26:1315–1337

Hewitson BC, Daron J, Crane RG, Zermoglio MF, Jack C (2013) Interrogating empirical-statistical downscaling. Clim Chang 122:539–554. doi: 10.1007/s10584-013-1021-z

IPCC (2014) Summary for policymakers. In: Field CB, Barros VR, Dokken DJ, Mach KJ, Mastrandrea MD, Bilir TE, Chatterjee M, Ebi KL, Estrada YO, Genova RC, Girma B, Kissel ES, Levy AN, MacCracken S, Mastrandrea PR, White LL (eds) Climate change 2014: impacts, adaptation, and vulnerability. Part a: global and sectoral aspects. Contribution of Working Group II to the Fifth Assessment Report of the Intergovernmental Panel on Climate Change. Cambridge University Press, Cambridge, pp 1–32

Kalnay E, Kanamitsu M, Kistler R, Collins W, Deaven D, Gandin L, Iredell M, Saha S, White G, Woollen J, Zhu Y, Chelliah M, Ebisuzaki W, Higgins W, Janowiak J, Mo KC, Ropelewski C, Wang J, Leetmaa A, Reynolds R, Jenne R, Joseph D (1996) The NCEP/NCAR 40-year reanalysis project. Bull Am Meteorol Soc 77:437–472

Katzfey KK, McGregor JL, Nguyen K, Thatcher M (2009) Dynamical downscaling techniques: impacts on regional climate change signals 18th World IMACS/MODSIM Congress. Cairns, Australia, 2009

Kim J, Waliser DE, Mattmann CA, Goodale CE, Hart AF, Zimdars PA, Crichton DJ, Jones C, Nikulin G, Hewitson B, Jack C, Lennard C, Favre A (2014) Evaluation of the CORDEX-Africa multi-RCM hindcast: systematic model errors. Clim Dyn 42:1189–1202. doi: 10.1007/s00382-013-1751-7

Kruger AC, Sekele SS (2013) Trends in extreme temperature indices in South Africa: 1962–2009. Int J Climatol 33:661–676. doi: 10.1002/joc.3455

Landman WA, Beraki A (2012) Multi-model forecast skill for mid-summer rainfall over southern Africa. Int J Climatol 32:303–314. doi: 10.1002/joc.2273

Landman WA, Goddard L (2002) Statistical recalibration of GCM forecasts over southern Africa using model output statistics. J Clim 15:2038–2055

Landman WA, Beraki A, DeWitt D, Lötter D (2014) SST prediction methodologies and verification considerations for dynamical mid-summer rainfall forecasts for South Africa. Water SA 40(4):615–622. doi: 10.4314/wsa.v40i4.6

Lazenby M, Landman WA, Garland R, DeWitt D (2014) Seasonal temperature prediction skill over southern Africa and human health. Meteorol Appl 21:963–974. doi: 10.1002/met.1449

Malherbe J, Landman WA, Olivier C, Sakuma H, Luo J-J (2014) Seasonal forecasts of the SINTEX-F coupled model applied to maize yield and streamflow estimates over north-eastern South Africa. Meteorol Appl 21:733–742. doi: 10.1002/met.1402

Maraun D, Wetterhall F, Ireson AM, Chandler RE, Kendon EJ, Widmann M, Brienen S, Rust HW, Sauter T, Themeßl M, Venema VKC, Chun KP, Goodess CM, Jones RG, Onof C, Vrac M, Thiele-Eich I (2010) Precipitation downscaling under climate change. Recent developments to bridge the gap between dynamical models and the end user. Rev Geophys 48:RG3003. doi: 10.1029/2009RG000314

Mason SJ, Tippett MK (2016) Climate predictability tool version 15.3. Columbia University Academic Commons, New York. doi: 10.7916/D8NS0TQ6

McGregor JL (2005) C-CAM: geometric aspects and dynamical formulation. CSIRO Atmospheric Research Technical Paper, No 70, 41.

McGregor JL (2015) Recent developments in variable-resolution global climate modelling. Clim Chang 129:369–380

McGregor JL, Dix MR (2001) The CSIRO conformal-cubic atmospheric GCM. In: Hodnett PF (ed) Proc. IUTAM Symposium on Advances in Mathematical Modelling of Atmosphere and Ocean Dynamics. Kluwer, Dordrecht, pp 197–202

McGregor JL, Dix MR (2008) An updated description of the conformal-cubic atmospheric model. In: Hamilton K, Ohfuchi W (eds) High resolution simulation of the atmosphere and ocean. Springer Verlag, Berlin, pp 51–76

Meehl GA, Covey C, Delworth T, Latif M, McAvaney B, Mitchell JFB, Stouffer RJ, Taylor KE (2007) The WCRP CMIP3 multi-model dataset: a new era in climate change research. Bull Am Meteorol Soc 88:1383–1394

Mitchell TD, Jones PD (2005) An improved method of constructing a database of monthly climate observations and associated high-resolution grids. Int J Climatol 25:693–712. doi: 10.1002/joc.1181

Mjelde JW, Thompson TN, Nixon CJ, Lamb PJ (1997) Utilising a farm-level decision model to help prioritise future climate prediction research needs. Meteorol Appl 4:161–170

Nguyen KC, Katzfey JJ, McGregor JL (2012) Global 60 km simulations with CCAM: evaluation over the tropics. Clim Dyn 39:637–654

Riphagen HA, Bruyère CL, Jordaan W, Poolman ER, Gertenbach JD (2002) Experiments with the NCEP regional eta model at the South African Weather

Bureau, with emphasis on terrain representation and its effect on precipitation predictions. Mon Weather Rev 130:1246–1263

Rummukainen M (2010) State-of-the-art with regional climate models. WIRES Clim Change 1:82–96. doi: 10.1002/wcc.8

Schmidt F (1977) Variable fine mesh in spectral global model. Beitr Phys Atmos 50:211–217

Thatcher M, McGregor JL (2009) Using a scale-selective filter for dynamical downscaling with the conformal cubic atmospheric model. Mon Weather Rev 137:1742–1752

Thatcher M, McGregor JL (2010) A technique for dynamically downscaling daily-averaged GCM datasets over Australia using the conformal cubic atmospheric model. Mon Weather Rev 139:79–95

Thornton PK, Jones PG, Ericksen PJ, Challinor AJ (2011) Agriculture and food systems in sub-Saharan Africa in a 4°C+ world. Phil Trans R Soc A 369:117–136. doi: 10.1098/rsta.2010.0246

Weaver SJ, Kumar A, Chen M (2014) Recent increases in extreme temperature occurrence over land. Geophys Res Lett 41:4669–4675. doi: 10.1002/2014GL060300